PROCEEDINGS OF SCIENCE

Locating the critical point of QCD phase transition by finite-size scaling

Yuanfang Wu[*†]
Institute of particle physics, Huazhong Normal university.
E-mail: wuyf@iopp.ccnu.edu.cn

Lizhu Chen
Institute of particle physics, Huazhong Normal university.

X.S. Chen
Institute of Theoretical Physics, Chinese Academy of Sciences, Beijing, China.

It is pointed out that in relativistic heavy ion collisions, critical related observable in the vicinity of critical point should follow finite-size scaling. The methods of finding and locating critical point are established for the first time by finite-size scaling and its critical characteristics, in particular, the fixed-point and straight-line behavior. As an application of the method, the critical behavior at RHIC data is demonstrated.

5th International Workshop on Critical Point and Onset of Deconfinement - CPOD 2009,
June 08 - 12 2009
Brookhaven National Laboratory, Long Island, New York, USA

[*]Speaker.

[†]This work is supported in part by the NSFC of China with project No. 10835005 and MOE of China with project No. IRT0624 and No. B08033.

PoS(CPOD 2009)036

1. Introduction

Lattice-QCD has predicted two phase transitions at finite temperature and density [1]. One is quark deconfinement, and the other one is chiral symmetry restoration. It has also been shown that both of them are crossover at vanishing baryon chemical potential $\mu_{\rm B}$ [2]. Much speculation from model investigation indicates that the crossover turns to be a true first-order phase transition for larger values of $\mu_{\rm B}$. In QCD phase diagram, the endpoint of the first order phase transition to analytical crossover is referred to as critical endpoint, or critical point [3]. However, it is still a difficult problem to determine the critical point from first principle of lattice calculation. Whether the critical points of these two phase transitions occur at the same or different critical temperature is unclear[4].

Locating the critical points is essential for mapping the QCD phase diagram [5]. The experiments of current Relativistic Heavy Ion Collider (RHIC) at BNL, the SPS at CERN, and future FAIR at GSI are aimed to produce the conditions which make the QCD phase transitions occur, and finally to locate the critical points. If they are in the region accessible to current relativistic heavy ion collisions, they could be discovered experimentally. But how to locate them from experimental observable has not been settled yet.

In relativistic heavy ion collisions, the size of the formed matter is limited. More central collision makes the overlapped area larger, and therefore the large number of strongly interacting nucleons. This makes the transition of quark deconfinement possible.

In infinite system, the critical related observable is divergent at critical point. But in finite system, this divergence can not be practically observed. It becomes finite and changes with system size. In the vicinity of critical point, the observable at different system sizes follow the finite-size scaling.

Finite-size scaling was proposed from phenomenological [6] and renormalization-group [7] theories, and was approved by the Monte Carlo simulations of various universal classes [8]. Finite-size scaling not only describe the behavior of the thermodynamic quantities in the vicinity of critical point, but also indicates the position of critical point and the values of critical exponents in infinite system.

It is found recently that the finite-size scaling holds not only for thermodynamic quantities like order-parameter, susceptibility, and so on, but also for various cluster sizes [9] and their fluctuations [10]. Therefore, the finite-size scaling of various critical related observable could be used to identify critical point and its critical exponents.

2. Locating critical point by finite-size scaling in relativistic heavy ion collisions

A critical related observable Q in relativistic heavy ion collisions is a function of incident energy $\sqrt{s}$ and system size L. Incident energy $\sqrt{s}$ is the controlling parameter, like temperature T, or external field h in thermodynamic systems. When L is much larger than the microscopic length scale and $\sqrt{s}$ is near the critical incident energy $\sqrt{s_c}$, the observable $Q(\sqrt{s},L)$ can be written in a finite-size scaling form [6, 7, 8]

$$Q(\sqrt{s},L) = L^{\lambda/\nu} F_Q(\tau L^{1/\nu}) \tag{2.1}$$

where $\tau = (\sqrt{s} - \sqrt{s_c})/\sqrt{s_c}$ is the reduced variable and λ is the critical exponent of the observable. ν is the critical exponent of the correlation length $\xi = \xi_0 \tau^{-\nu}$. Finite-size scaling indicates that the observable at different system sizes can be re-scaled to an identical scaling function F_Q with scaled variable $\tau L^{1/\nu}$.

When incident energy $\sqrt{s} \neq \sqrt{s_c}$, the scaled variable $\tau L^{1/\nu} \neq 0$ and the scaling function F_Q changes with incident energy and system size L. At $\sqrt{s} = \sqrt{s_c}$, the scaled variable ($\tau L^{1/\nu} = 0$) is independent of system size L, and scaling function,

$$F_Q(0) = Q(\sqrt{s_c}, L) L^{-\lambda/\nu}, \tag{2.2}$$

becomes a constant. In the plot of $Q(\sqrt{s}, L)L^{-\lambda/\nu}$ *vs.* $\sqrt{s}$ for different system size L, the critical point $[\sqrt{s_c}, F_Q(0)]$ is a *fixed point*, where all curves of $Q(\sqrt{s}, L)L^{-\lambda/\nu}$ with respect to $\sqrt{s}$ at different size L converge to. Reversely, the appearance of fixed point indicates the existence of critical point.

If the critical exponent $\lambda = 0$, the fixed point can be obtained directly from the incident energy dependence of this observable at different system sizes, like Binder cumulant ratio [11], which is used widely in determining critical point in thermodynamic system with finite size.

If the critical exponent $\lambda \neq 0$ and is unknown, the fixed point can be found by investigating the incident energy dependence of $Q(\sqrt{s}, L)L^{-a}$ at different system sizes. If a fixed point is observed at $a = a_0$ when tuning the parameter $-a$ from $-\infty$ to ∞, then the postion of fixed point indicates the critical incident energy and a_0 is the ratio of critical exponents, i.e., $\lambda/\nu = a_0$.

The critical point can also be found from the system size dependence of the observable. Taking logarithm in the both sides of Eq. (2.1), it becomes

$$\ln Q(\sqrt{s}, L) = \lambda/\nu \ln L + \ln F_Q(\tau L^{1/\nu}). \tag{2.3}$$

At critical point $\tau = 0$, the second term is constant and $\ln Q(\sqrt{s_c}, L)$ with respect to $\ln L$ becomes a straight line with slope equal to the ratio λ/ν. When system is away from the critical point, the second term depends on the system size and $\ln Q(\sqrt{s}, L)$ with respect to $\ln L$ deviates from a straight line.

In relativistic heavy ion collisions, the critical incident energy and the ratio of critical exponent are both unknown. In this case, we have firstly to examine whether there is any fixed-point and best straight-line behavior. If there is a fixed-point, the corresponding position of the fixed-point and parameter $a = a_0$ will determine the critical incident energy and the ratio of critical exponent, respectively. Then around the fixed-point, the best scaling (Eq.(1)) fitting for all data at different system sizes will finally determine the critical exponent ν, which identifies the universality class of the critical point. So finite-size scaling, and its critical characteristics, fixed-point and straight-line behavior, provide a well-defined method for finding and locating the critical point in the experiments of relativistic heavy ion collisions.

3. Critical bahaviour of p_t and normalized p_t correlations at RHIC energies

It is interesting to see if there is any fixed-point and straight-line behavior at RHIC data. In relativistic heavy ion collision, various theoretical works predict the significant dynamic event-by-event fluctuations and correlations in apparent temperature, mean transverse momentum, multiplicity, and conserved quantities at critical point [12]. The centrality dependence of p_t correlation for

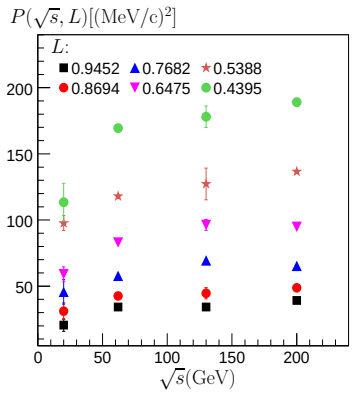

Figure 1: (Color online) The energy dependence of p_{t} correlations at different sizes L (or centralities). Data come from RHIC/STAR [13].

Au+ Au collisions at 4 incident energies are well presented [13]. We take it as an example. But it should be mentioned that the errors of the data at $\sqrt{s} = 20$ GeV are much larger than that at other incident energies. The p_{t} correlation is defined as

$$P(\sqrt{s},L) = \frac{1}{N_{\mathrm{e}}} \sum_{k=1}^{N_{\mathrm{e}}} \frac{\sum_{i=1}^{N_k} \sum_{j=1,i\neq j}^{N_k} (p_{\mathrm{t},i} - \langle\langle p_{\mathrm{t}}\rangle\rangle)(p_{\mathrm{t},j} - \langle\langle p_{\mathrm{t}}\rangle\rangle)}{N_k(N_k-1)} \tag{3.1}$$

where N_{e} is the number of event, $p_{\mathrm{t},i}$ is the transverse-momentum of the i-th particle, and N_k is the total number of particles in the k-th event. $\langle\langle\ldots\rangle\rangle$ is overall event average transverse momentum.

If the system has a critical point at incident energy $\sqrt{s_c}$ and corresponding critical behavior are survived after final state interactions, the p_{t} correlation in the vicinity of $\sqrt{s_c}$ could be written in a scaling form

$$P(\sqrt{s},L) = L^{\lambda/\nu} F_P(\tau L^{1/\nu}) \tag{3.2}$$

where λ is the critical exponent of p_{t} correlation.

The size of the formed matter is mainly limited by the size of overlapping area, which is proportional to the number of participant nucleons and is quantified as centrality. So the initial mean size of the formed matter can be approximately estimated by the square root of participants, $\sqrt{N_{\mathrm{part}}}$. We choose dimensionless (or relative) size

$$L = \sqrt{N_{\mathrm{part}}}/\sqrt{2N_{\mathrm{A}}} \tag{3.3}$$

as initial size of the system. Where N_{A} is the number of nucleons of incident nucleus.

In general, the system size L' at transition is larger than the initial size L and is a monotonically increasing function of L, e.g., $L' = cL^{1+\delta}$ with $\delta \geq 0$. If we use L' instead of L in finite-size scaling in Eq. (3.2), the scaling exponents will be modified, but the position of critical point does not change. The most interesting thing is to find the position of critical point. So we will use the initial size L in finite-size scaling in the following discussions.

Firstly, we change the centrality dependence of p_{t} correlation at different collision energies [13] to the incident energy dependence at different centralities. The results are shown in

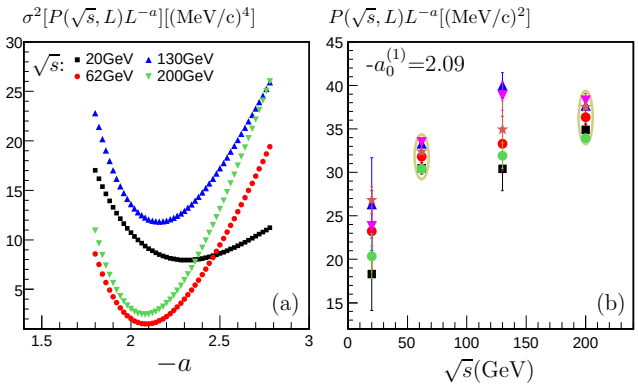

Figure 2: (Color online) (a) The width of $P(\sqrt{s},L)L^{-a}$ distribution for varying parameter $-a$ at 4 given incident energies, $\sigma^2[P(\sqrt{s},L)L^{-a}]$. (b) p_{t} correlation multiplied by the factor, $L^{-a_0^{(1)}}$, with $-a_0^{(1)} = 2.09$.

Fig. 1. Since in the most peripheral collisions, the size of the formed matter is too small to be inside the asymptotic region of finite-size scaling, we choose six centralities at mid-central and central collisions to do the analysis. The initial sizes of the formed systems at the 6 centralities are listed in the legend of Fig. 1. It is clear that at a given incident energy, the correlation strength increases with the decrease of system size. The influence of finite size is obvious.

Then we multiply $P(\sqrt{s},L)$ by a size factor L^{-a} with $-a$ varying from $-\infty$ to ∞. The width of $P(\sqrt{s},L)L^{-a}$ distribution at a given incident energy quantifies whether those points of different sizes are close to each other. It is defined as $\sigma^2[P(\sqrt{s},L)L^{-a}] = \sigma^6_{i=1}[P(\sqrt{s},L_i) - \langle P(\sqrt{s},L)\rangle]^2$. For an ideal fixed point, $\sigma^2_{min}[P(\sqrt{s},L)L^{-a}] = 0$. The $\sigma^2[P(\sqrt{s},L)L^{-a}]$ for different values of parameter $-a$ at 4 incident energies are shown in Fig. 2(a). Where the error of $\sigma^2[P(\sqrt{s},L)L^{-a}]$ is not provided due to the shortage of higher order moments of p_{t} correlations. It is interesting to see that there is a minimum value for varying parameter $-a$ at each given incident energy. The minimum values at $\sqrt{s} = 62$ and 200 GeV are less than 2 and much smaller than that at $\sqrt{s} = 20$ and 130 GeV. The slopes of minimum valley at $\sqrt{s} = 62$ and 200 GeV are much steeper than that at other two energies.

This shows that at $\sqrt{s} = 62$ (or 200) GeV, all points of different sizes move firstly toward each other, then well converge at $-a_0^{(1)} = 2.09$ (or $-a_0^{(2)} = 2.08$), and finally move apart again from each other. The results for $-a_0^{(1)} = 2.09$ are presented in Fig. 2(b), where the errors come from the p_{t} correlations only, and the errors of centrality are not included. While at incident energies $\sqrt{s} = 20$ (or 130) GeV, the points of different sizes never move close to each other as those at $\sqrt{s} = 62$ (or 200) GeV do. So there are two fixed points around $\sqrt{s} = 62$ and 200 GeV.

In order to confirm the position of fixed points, we study the $\ln L$ dependence of $\ln P(\sqrt{s},L)$ for 4 incident energies, respectively. A parabola fit, $c_2(\ln L)^2 + c_1 \ln L + c_0$, is used at each incident energy. The better straight-line behavior should result in smaller $|c_2|$ and larger ratio of $|c_1/c_2|$. The fit parameters, c_2 and c_1, for 4 incident energies are listed in Tab. 1. It shows that the better straight-line behavior happen to be at $\sqrt{s} = 62$ and 200 GeV, i.e., at the same incident energies of the fixed points. The data at these two incident energies can be well fitted by the straight lines with slopes $a_0^{(1)}$ and $a_0^{(2)}$, respectively. The results are shown in Fig. 2(a). While, the data at $\sqrt{s} = 20$ and 130 GeV are better fitted by parabola and shown in Fig. 2(b).

Table 1: Parameters of parabola fits.

$\sqrt{s}$(GeV)	20	62	130	200
$\|c_2\|$	1.86± 0.93	0.6 ± 0.09	1.56± 0.41	0.77± 0.1
$\|c_1\|$	3.9±0.89	2.59± 0.09	3.43± 0.41	2.74±0.1

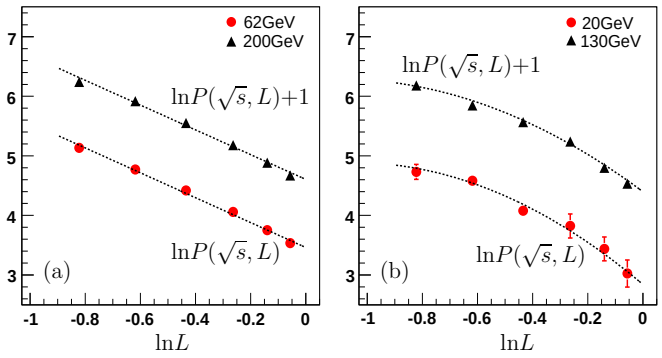

Figure 3: (Color online) Double-log plots of p_t correlation with respect to size, (a): straight-line fits with slopes $a_0^{(1)}$ and $a_0^{(2)}$ obtained by fixed points, and (b): parabola fits.

The same analysis has been done for the normalized p_t correlation, where the normalization is for overall event average p_t [13]. It shows exactly the same best fixed-point and straight-line behavior at $\sqrt{s} = 62$ and 200 GeV. Their ratios of critical exponents are both 1.1, i.e., $-a_0^{(1)} = -a_0^{(2)} = 1.1$.

So the critical incident energies are most probably around $\sqrt{s} = 62$ and 200 GeV, rather than near $\sqrt{s} = 20$ and 130 GeV. The same analysis for other critical related observable, such as the fluctuation of mean p_t per event, the moments of multiplicity [12], the ratio of K to π [14], the third order moments of conserved charges [15] and so on, will be helpful in confirming the observed results. The incident energy and centrality dependence of those observable are called for.

If there were additional collisions around $\sqrt{s} = 62$ and 200 GeV, we could determine precisely the critical incident energy and critical exponents by the best fitting of the finite-size scaling function. This is impossible at present since there are only two collision energies in addition to the critical ones, and they could be outside of the asymptotic region where finite-size scaling holds.

Two critical incident energies, $\sqrt{s} = 62$ and 200 GeV, are both within the range of critical points estimated by lattice calculation [16]. The fact that the ratios of critical exponents at two critical points are close is consistent with current theoretical estimation, which shows that all critical exponents of the deconfinement transition are very close to that of chiral symmetry restoration. Where the deconfinement and chiral symmetry restoration transitions are supposed to be the same universities as the 3-dimensional Ising model [17], and the 3-dimensional O(4) model with spin symmetry [18], respectively.

4. Summary

To the summary, we pointed out that in relativistic heavy ion collisions, the finite-size effects

of the formed matter is not negligible. The critical related observable should follow the finite-size scaling. The methods of finding and locating critical point of QCD phase transition are established for the first time by finite-size scaling and its characteristics at critical point, in particular, the fixed point and straight line behavior. As application of the method, the critical behavior of $p_{\rm t}$ correlation and its normalized one from RHIC/STAR are demonstrated. The fixed-point and the best straight-line behavior are observed around $\sqrt{s} = 62$ and 200GeV.

The confirmation of this observation requires the efforts from both theoretical and experimental sides. From experimental side, it is proposed to get more and better data on other critical related observable, and a few additional collisions around $\sqrt{s} = 62$ and 200 GeV. Then we can more precisely determine the critical points and critical exponents of QCD phase transitions.

Acknowledgments

The authors are grateful to Prof. Liu Lianshou, Dr. Xu Nu, Dr. Li Liangsheng, Prof. Dr. Hou Defu and Prof. Li Jiarong for very helpful discussions.

References

[1] J. C. Collins, M. J. Perry, Phys. Rev. Lett. **34**, 1353 (1975); B. A. Freedman, L. D. Lerran, Phys. Rev. **D 16**, 1196 (1977); E. V. Shuryak, Phys. Lett. **B 107**, 103 (1981).

[2] Y. Aoki, G. Endrodi, Z. Fodor, S. D. Katz, K.K. Szabo, Nature **443**, 675 (2006); Y. Aoki, Z. Fodor, S.D. Katz, K.K. Szabo, Phys. Lett. **B 643**, 46 (2006).

[3] Z. Fodor and S. D. Katz, J. High Energy Phys., 050 (2004); Z. Fodor, S. D. Katz, and K. K. Szabo, Phys. Lett. **B 568**. 73 (2003).

[4] Karsch F. And Lutgemeier M., Nucl. Phys. **B 550**, 449 (1999); Karsch F., Lecture Notes Phys. **583**, 209 (2002), hep-lat/0106019; Y. Aoki, Z. Fodor, S. D. Katza, and K. K. Szabo, Phys. Lett. **B 643**, 46 (2006); Ágnes Mócsy, Francesco Sannino and Kimmo Tuominen, J. Phys. **G 30**, S1255 (2004).

[5] Adrian Cho, Science, **312**, 190 (2006).

[6] M. E. Fisher, in Critical Phenomena, Proceedings of the International School of Physics ąřEnrico Fermi,ąś Course 51, edited by M. S. Green (Academic, New York, 1971).

[7] E. Brézin, J. Phys. (Paris) **43**, 15 (1982).

[8] X. S. Chen, V. Dohm, and A. L. Talapov, Physica **A 232**, 375 (1996); X. S. Chen, V. Dohm, and N. Schultka, Phys. Rev. Lett. **77**, 3641 (1996). A. Esser, V. Dohm, and X. S. Chen, Physica **A 222**, 355 (1995).

[9] Li Liangsheng and X.S. Chen (to be published).

[10] Chen Lizhu, Li Liangsheng, X.S. Chen and Wu Yuanfang (to be published).

[11] K. Binder, Z. Phys. **B 43**, 119 (1981).

[12] M. A. Stephanov, K. Rajagopal, and E. Shuyak, Phys. Rev. Lett. **81**, 4816 (1998); H. Heiselberg, Phys. Rept. **351**, 161 (2001).

[13] J. Adams, et. al. (STAR collaboration), Phys. Rev. **C 72**, 044902 (2005).

[14] M. A. Stephanov, Phys. Rev. Lett. **102**, 032301 (2009).

[15] Masayuki Asakawa, Shinji Ejiri, Masakiyo Kitazawa, nucl-th 0904.2089.

[16] Y. Aoki, Z. Fodor, S. D. Katza, and K.K. Szabo, Phys. Lett. **B 643**, 46 (2006); F. Karsch, PoS CFRNC2007, arXiv: 0711.0661; M. Stephanov, arXiv: hep-lat:0701002.

[17] Jorge Garcá, Julio A. Gonzalo, Physica **A 326**, 464 (2003).

[18] Jens Braun1 and Bertram Klein, Phys. Rev. **D 77**, 096008 (2008).